CICE2023 Rio de Janeiro – Brazil 11TH INTERNATIONAL CONFERENCE ON FRP COMPOSITES IN CIVIL ENGINEERING

DESIGN AND OPTIMIZATION OF A GFRP AND STEEL HYBRID PRESTRESSED SFRC BEAM BASED ON NUMERICAL AND ANALYTICAL APPROACHES

Kamyar B. Shahrbijari, ISISE, ARISE, University of Minho, Portugal, kamyar.ba@civil.uminho.pt
Joaquim A. O. Barros, ISISE, ARISE, University of Minho, Portugal, barros@civil.uminho.pt
Isabel B. Valente, ISISE, ARISE, University of Minho, Portugal, isabelv@civil.uminho.pt

ABSTRACT
Due to corrosion immunity, GFRP bars can be used in combination with steel bars and disposed in arrangements that take advantage of their specific properties. Since steel stirrups are the most susceptible to corrosion, significant advantages can be obtained with their replacement by fiber reinforcement, using Steel Fiber Reinforced Concrete (SFRC), which also allows to decrease the thickness of the beam's web. In addition, prestressing the flexural reinforcement increases the service load-carrying capacity of the beams and their shear strength. This study highlights the flexural performance of hybrid prestressed GFRP-Steel SFRC beams considering the optimum design provided with the use of a genetic algorithm (GA) on simply supported I-shaped beams. The results show that the proposed GA-based optimization procedure provides an effective approach to obtain the balanced reinforcement ratio for these types of beams.

KEYWORDS
Fiber reinforced concrete; Hybrid GFRP-Steel reinforcement; Prestress; optimum design; Genetic algorithm; moment-curvature.

INTRODUCTION
In aggressive environments, Fiber Reinforced Polymer (FRP) bars, such as glass FRP (GFRP) bars, have been used to replace steel bars as a flexural reinforcement (El-Nemr et al., 2018; Pan & Yan, 2021) with the objective of reducing the risk of steel reinforcement corrosion in reinforced concrete (RC) members. The advantages of using FRP bars in concrete structures are their high strength-to-weight ratio, nonsusceptibility to corrosion, nonconducting and nonmagnetic capacity, good chemical resistance, and high tensile strength (Chen et al., 2020; Gemi et al., 2019). However, the GFRP bars present a low modulus of elasticity and a brittle tensile rupture, posing concerns in terms of accomplishing serviceability limits (SLS), such as deflection and crack width (Spagnuolo et al., 2021). The susceptibility of GFRP bars to fire events is also another concern and an adequate steel reinforcement ratio is required (Rosa et al., 2019). The use of a hybrid FRP-Steel reinforcement can be a solution (Lu et al., 2022; Taheri et al., 2020) to overcome these concerns if steel and GFRP bars are appropriately disposed.
In recent decades, there has been significant interest in using steel fiber reinforced concrete (SFRC) to improve the flexural and shear behavior of RC beams (Adel et al., 2022; Ahmed & Chidambaram, 2022; Barros et al., 2022; Salehian & Barros, 2017). In terms of shear performance, the fibers bridging the shear cracks introduce an extra parcel of shear resistance due to the fibers' pullout and aggregate interlock shear-resisting mechanisms (Matos et al., 2020).
The design of hybrid GFRP-Steel prestressed SFRC beams requires considerable calculations and data processing, and their structural optimization is a challenging task.
This study aims to optimize the hybrid prestressed flexural reinforcement of a SFRC beam. An I-shape simply supported beam which includes prestressed GFRP and Steel bars as flexural reinforcements is considered. The web thickness of the I-shape is minimized by using steel fibers instead of steel stirrups. For the optimization of the structural performance of this beam, the balanced reinforcement ratio (BRR) of the prestressed GFRP and Steel bars was determined, by using a genetic algorithm (GA). In a hybrid FRP-Steel RC beam, theoretically, the BRR assures the simultaneous occurrence of concrete crushing, steel yielding, and FRP tensile rupture. However, due to the different properties of these materials, this situation is nearly impossible. Therefore, for providing a ductile failure mode, the BRR in this scenario assures the simultaneous occurrence of concrete crushing and FRP bars tensile rupture, while the steel

reinforcement has already yielded. GA is an iterative computer-based method that is commonly adopted for solving stochastic search and optimization problems.
The design of complex structures such as hybrid GFRP-Steel prestressed SFRS beams requires a large amount of calculation and data processing, and its optimization becomes one of the most challenging tasks for most structural designers. This study shows that the proposed methodology using GA is a good alternative to traditional design methods, can be applied to any cross-sectional shape and any reinforcement arrangement, and will facilitate the design and usage of these types of structural elements. A computer program coded in C# was developed to assist in this optimum design process, and its potentialities are demonstrated in a design example.

METAHEURISTIC OPTIMIZATION ALGORITHMS

In the field of optimization, metaheuristic algorithms are used in search procedures to find good solutions for complex and challenging problems. The genetic algorithm (GA) is an example of a metaheuristic algorithm that is used to find solutions for problems that are difficult to solve using traditional algorithms. There are a number of advantages of the genetic algorithm over traditional ones, including the good ability to make a global search over a large solution space, easy to understand, and the capability of multi-objective optimization.
A GA is a numerical optimization technique based on Darwin's theory that uses the principles of natural selection (Aydın & Ayvaz, 2010). A GA first creates a population of individuals (designs) on a random basis and then begins to search within them. GA uses four main operators, including, initial population, selection, crossover, and mutation, to direct the population toward the optimum solution.

OPTIMUM DESIGN OF PRESTRESSED SFRC BEAM

In this study, a model is proposed to determine the nominal flexural strength (M_n) of a beam flexurally reinforced with a prestressed GFRP-Steel bars arrangement (hybrid reinforcement). A GA was adopted to determine the BRR for the structural optimization of a simply supported prestressed I-shaped SFRC beam with a span length of 4 meters, according to the adopted design criteria for this type of beam. The geometry of the beam's cross-section for the numerical example was obtained from (Mazaheripour et al., 2016). Fig. 1a shows the geometry of the proposed beam.

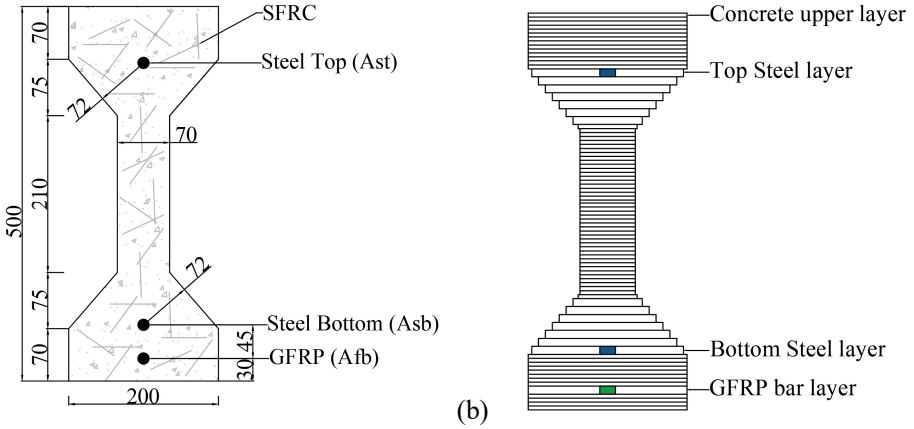

Fig. 1 Beam cross-section: (a) Geometry and disposition of the reinforcements (dimension in mm) (b) Layered model

Flexural design

General considerations

At a typical concrete beam with prestressed steel tendons, the deformation due to external loads is elastic until concrete cracking initiation, and beam's failure occurs due to the tensile rupture of the steel tendon (after some plastic deformation of the steel) or concrete crushing. The main difference between the behavior of a beam prestressed with FRP and a beam prestressed with steel is the type of failure of the prestressed reinforcement, which in the case of FRP is brittle and without any plastic incursion. This can reduce significantly the ductility of the beam at its failure.

Regarding the BRR to be determined, it should be noted that a reinforcement solution below the BRR results in tensile rupture of FRP bars before concrete crushing (under-reinforced i.e. $\varepsilon_f = \varepsilon_{fu}\ and\ \varepsilon_c < \varepsilon_{cu} = 0.0035$), while a reinforcement ratio above the BRR conducts to concrete crushing without occurring tensile failure of the FRP bars (over-reinforced i.e. $\varepsilon_f < \varepsilon_{fu}\ and\ \varepsilon_c > \varepsilon_{cu} = 0.0035$).
In this study, to evaluate the flexural capacity of the section during the optimization process, a moment-curvature analysis is performed using DoCros software (Basto & Barros, 2008). DoCros can analyze sections of irregular shape and size, composed of different types of materials subjected to an axial force and variable curvature. DoCros has a wide database of constitutive laws for the simulation of monotonic and cyclic behavior of cement-and polymer-based materials, and steel bars (Varma et al., 2012).

Design parameters

Maximum allowable stresses

According to the AASHTO Bridge design specification (Aashto, 2012) the maximum allowable initial prestress for Low Relaxation Strands is $0.70 f_{pu}$, where f_{pu} is the ultimate tensile strength of the steel strand.

The stress limitations of FRP bars are based on the creep rupture characteristics of the rods for any given service life. The available research indicates that stress levels for GFRP rods must be limited to 40% of their guaranteed tensile strength f_{fu} to ensure adequate safety against failures due to pulling and creep rupture (Rossini & Nanni, 2019).

Prestress losses

Losses of prestress are caused by slippage between reinforcements and surrounding concrete after releasing the prestressing jack, deformation of the anchorages, and concrete shrinkage and creep. Loss of prestressing can be determined by recording, with strain gauges or similar sensors, the evolution of the strain field in the reinforcements up to its stationarity. Prestress losses of 10% and 14% in steel and GFRP tendons, respectively, were reported in a hybrid pre-tensioned beam (Mazaheripour et al., 2016).

Material properties

In this study, a C40/50 SFRC strength class was adopted. Material properties considered in the numerical simulations are obtained from an experimental test reported elsewhere (Shahrbijari et al., 2020). An inverse analysis was performed for determining the tensile stress versus tensile strain diagram. This was done by fitting, with the minimum error, the load versus the crack mouth opening displacement (CMOD) registered experimentally in SFRC notched beams (Mazaheripour et al., 2016). The stress-strain diagrams adopted for modeling the behavior of the adopted materials are represented in Fig. 2, and the values of the variables defining these diagrams are provided in Table 1. By using these diagrams in DoCros software, the moment-curvature of the beam's cross-section is determined.

Table 1 Properties of the parameters defining the constitutive laws of the SFRC

SFRC Compression								
$f_{cc}(MPa)$	ε_{cc}	ε_{ccr}	$E_c(GPa)$					
52	0.0023	0.0035	31					
Tension								
$f_{ct1}(MPa)$	$f_{ct2}(MPa)$	$f_{ct3}(MPa)$	$f_{ct4}(MPa)$	$\varepsilon_{ct1}(\%)$	$\varepsilon_{ct2}(\%)$	$\varepsilon_{ct3}(\%)$	$\varepsilon_{ct4}(\%)$	$\varepsilon_{ct5}(\%)$
2.1	3.15	2.17	1.94	0.01	0.05	2.5	3.5	5

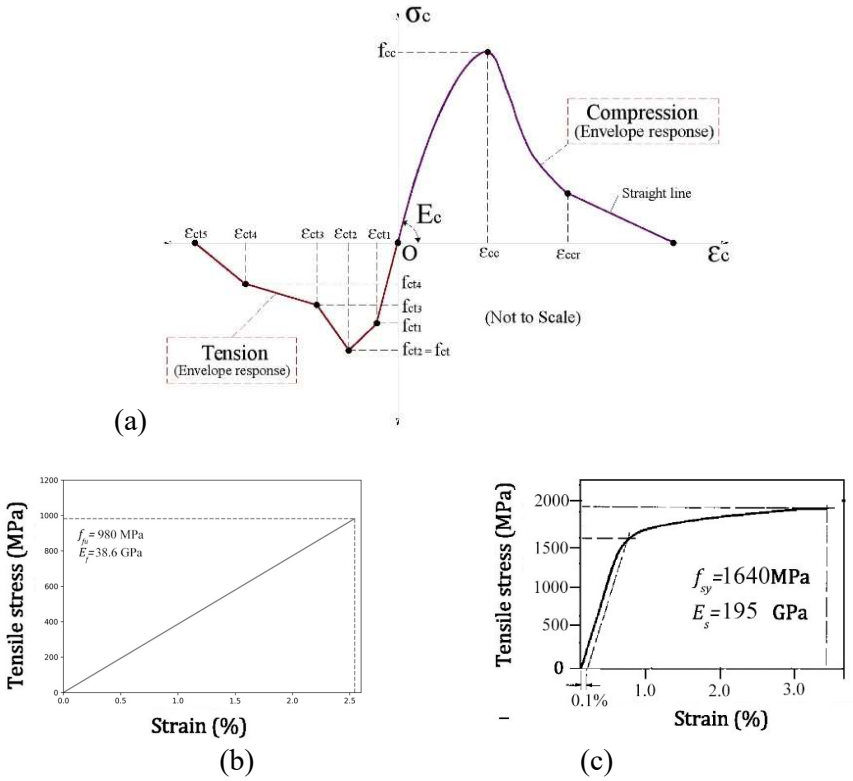

Fig. 2 Material properties used in the analysis of the beam: (a) Compressive and tensile stress-strain of SFRC; (b) and (c) tensile stress-strain of GFRP bars and steel strand, respectively

Additionally, Fig. 2b and Fig. 2c show the tensile stress-strain diagram of the GFRP and steel rebars, respectively. The f_{fu} is the guaranteed tensile strength of a helically wrapped (HW) GFRP rebar. For the steel strand, the ultimate tensile stress is 1860 MPa, while yielding stress (f_{sy}) of 1640 MPa was obtained at a tensile strain of 0.1% (proof stress, $f_{p0.1k}$).

Design variables

The design variables considered in this study are the cross-section areas of the reinforcement which are needed to obtain the BRR of the given beam's section. The configuration of the reinforcements is demonstrated in Fig. 1a in which A_{st} and A_{sb} are the cross-sectional area of the top and bottom steel reinforcements, respectively, while A_{fb} is the cross-sectional area of the GFRP reinforcement.

In the numerical model, a constant prestress level, by considering the prestress losses, is assigned as pre-strain to the corresponding layers for GFRP rebars and steel tendons at the initiation of the analysis. The prestress level adopted for the steel tendons and GFRP rebars was 60% and 26% of the corresponding material's tensile strength, respectively.

Sectional analysis and flexural capacity prediction

The geometry of the beam's cross-section and arrangement of the reinforcements are illustrated in Fig. 1a. To maximize the internal arm, the GFRP bars are located at the lowest layer of reinforcement, near the outer tensile surface, with the smallest concrete cover thickness required to transfer their relatively high stresses taking into account the limitation given by the bond performance of these bars (Mazaheripour et al., 2013). For the second layer of reinforcement in the tensile zone of the hybrid beam, the steel tendon is positioned with maximum concrete cover thickness from all sides of beam surfaces for providing proper protection against corrosion. To prevent cracks on the top beam's web, the maximum tensile strain generated by the high level of prestressing of GFRP and steel reinforcement at the bottom beam's web is controlled by applying an additional prestressed steel tendon in the top beam's web.

The flowchart of the proposed design methodology of a hybrid prestressed SFRC beam is shown in Fig. 3. A sectional analysis using DoCros has been used to determine the nominal flexural strength of a beam.

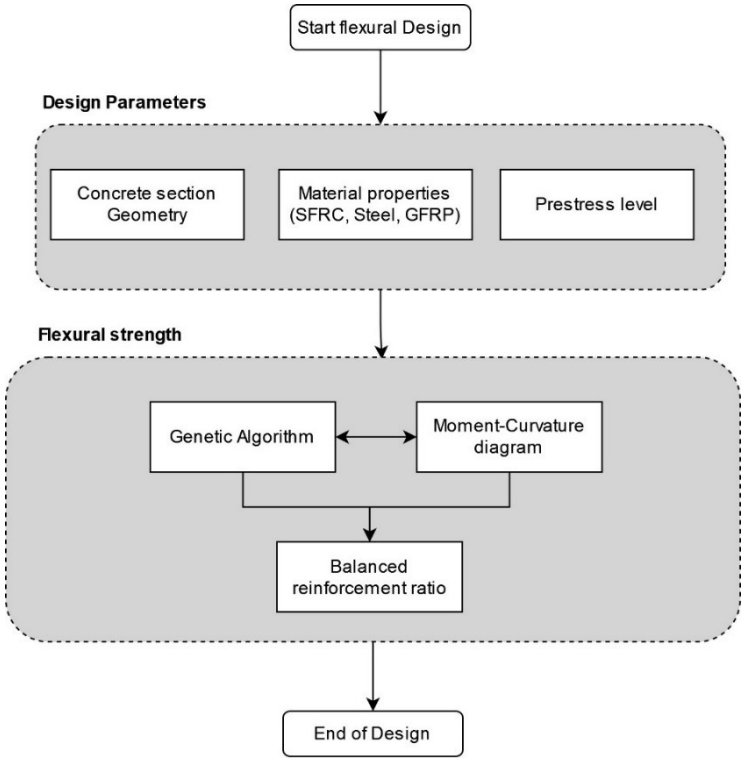

Fig. 3 Flowchart of the design methodology of a hybrid prestressed SFRC beam

In DoCros, an increment of strain is imposed in a selected layer up to a maximum limit, by determining the depth of the neutral axis that assures the force equilibrium of the cross-section. For each equilibrium state, the strain and stress in each layer are determined, as well as the moment-curvature of the section. For the model, the cross-section is discretized in layers of 5 mm thickness for the web, top, and bottom flanges, and 10 mm thickness for the web-flange transition zones (Fig. 1b).

The reinforcements are applied in three layers, as shown in Fig. 1b. The GFRP concrete cover is 20 mm, while the minimum concrete cover for steel tendons at the top and bottom layers is 72 mm.

Design methodology for the flexural design of the beam using GA

GA is employed to obtain the reinforcement cross-section areas at balanced conditions. The flowchart of the proposed optimization algorithm using GA is presented in Fig. 4, which shows that at each iteration of GA, the areas of reinforcements (A_{st}, A_{sb}, and A_{fb}, Fig. 1b) are estimated. Then the input data file of the DoCros model is updated with the new cross-sectional area of A_{st}, A_{sb}, and A_{fb}, and DoCros is executed by determining the strains and stresses in each layer, as well as the moment-curvature.

The design of the prestressed beam is performed in two stages. First, the strain at the upper layer of concrete after applying the prestress force is measured as a constraint to prevent cracking. A crack in concrete happens when the tensile strain in concrete exceeds, with a certain tolerance, the concrete cracking strain. Therefore, the strain on the concrete top surface should be less than the concrete cracking strain ($\varepsilon_c < \varepsilon_{ct1}$).

Then, the design criteria are checked for the failure of the prestressed beam. In this stage, the design criteria checked in each interaction of the GA are composed of the following conditions:

1) The strain in the concrete top surface should attain the concrete crushing strain ($\varepsilon_{cu} = 0.0035$);
2) Tensile strain in the GFRP reinforcement should attain its tensile rupture strain (ε_{GFRPu});
3) Tensile strain in the bottom steel reinforcement should be higher than its yield strain (ε_{sy}).

When these three conditions are verified, a possible solution for the BRR is determined, and the flexural capacity already obtained with DoCros is considered for achieving the optimum BRR solution (the one that assures the maximum resisting bending moment).

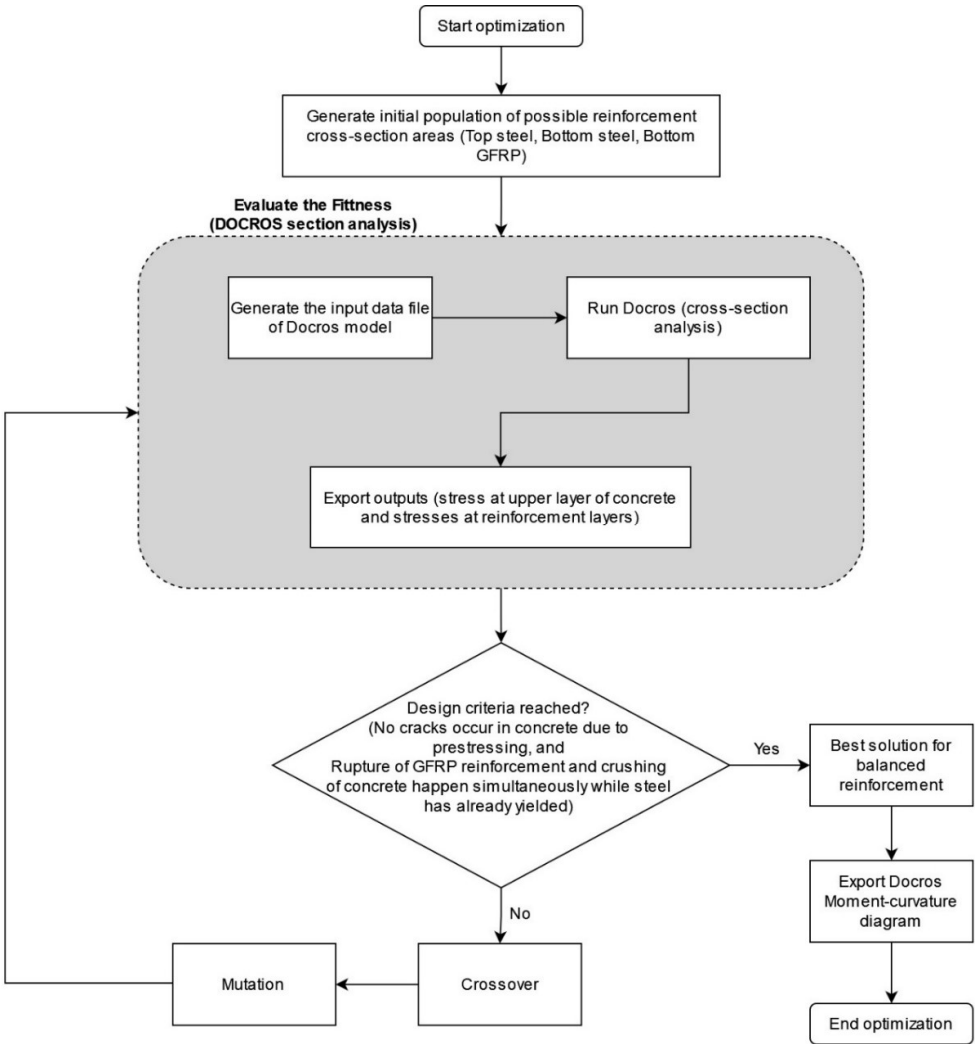

Fig. 4 The flowchart of the proposed optimization algorithm using GA

GA parameters selection

In the proposed framework, the genetic algorithm is implemented through the GeneticSharp library (Giacomelli, 2018), available on GitHub (Giacomelli, 2018). A software package was been developed in C# with this library to perform the optimization of the numerical example. GA consists of five phases: initial population, fitness, selection, crossover, and mutation. The phases of GA are described in the following sections, and more details can be found in (Mirjalili, 2019).

The GA starts with a random initial population and uses Gaussian random distribution to search for regions of interest. This population consists of various possible solutions for the rebars' cross-section areas (A_{st}, A_{sb}, A_{fb}). While a large population might slow down a GA, a smaller population might not provide enough mating opportunities. The minimum and maximum cross-section areas of design variables (A_{st}, A_{sb}, A_{fb}) are defined as 20 mm^2 to 1000 mm^2 respectively.
The fundamental goal of the initialization step is to distribute the solutions as uniformly as possible throughout the search space.

The fitness function determines the fitness of each possible solution (a set of A_{st}, A_{sb}, A_{fb}) generated within the GA, to assure the BRR condition. Hence, the fitness is based on the compressive strain in the concrete top surface, which should be as close as possible to the concrete ultimate compressive strain (ε_{cu}), on the tensile strain in the GFRP, which should be as close as possible to the GFRP ultimate tensile strain (ε_{GFRPu}), and on the tensile strain in the bottom steel reinforcement, which should exceed the yield strain (ε_{sy}), but never attaining its tensile rupture strain. The fitness function is defined as the sum of these differences according to Eq. 1 and Eq. 2:

$$\begin{cases} err_1 = \left|\varepsilon_{ConcreteTopSurface} - \varepsilon_{cu}\right| \\ err_2 = \left|\varepsilon_{BottomSteel\,\mathrm{Reinforcement}} - \varepsilon_{sy}\right| \\ err_3 = \left|\varepsilon_{GFRP\,\mathrm{Reinforcement}} - \varepsilon_{GFRPu}\right| \end{cases} \quad \text{Eq. 1}$$

$$Fitness = err_1 + err_2 + err_3 \quad \text{Eq. 2}$$

Therefore, the lower fitness value will be a better solution for the problem.

Once the generated variables (A_{st}, A_{sb}, A_{fb}) are not significantly different from the previous generation, the algorithm can be terminated. In this study, the GA is terminated when the fitness function tends to zero with the maximum resisting bending moment, which shows that the cross-section has a balanced reinforcement ratio.

Flexural design results and discussion

The design values and corresponding nominal flexural strength of the possible optimum solution of the algorithm (BRR condition and assure the maximum flexural capacity) are given in Table 2. It should be noted that based on the definition of BRR for hybrid reinforcement and due to the stochastic search of GA, the output may not provide a unique solution for reinforcement cross-section areas in all generation possibilities. In this study, the optimum solution has been reported based on the minimum balanced reinforcement ratios which provide the maximum flexural capacity.

Table 2 Values of design variables for the hybrid beam considered in the numerical example

A_{st}	21 (mm^2)
A_{sb}	152 (mm^2)
Tensile steel tendon reinforcement ratio (ρ_{sb})	0.27 (%)
A_{fb}	173 (mm^2)
GFRP bar reinforcement ratio (ρ_{fb})	0.31 (%)
The stress of tensile steel tendon at concrete crushing	1670 (MPa)
Nominal Flexural capacity	210.4 (kN.m)

Fig. 5 presents the evolution graph of the GA to obtain the BRR of a hybrid SFRC beam. The continuous line represents the evolution of the best solution (a set of A_{st}, A_{sb}, A_{fb}) of the generations obtained from Eq. 2. It can be seen that the fittest variables (reinforcement cross-section areas at BRR) of the generations are converging (crushing of concrete and rupture of GFRP bars occurred simultaneously while the steel strand is already yielded) after 25 generations.

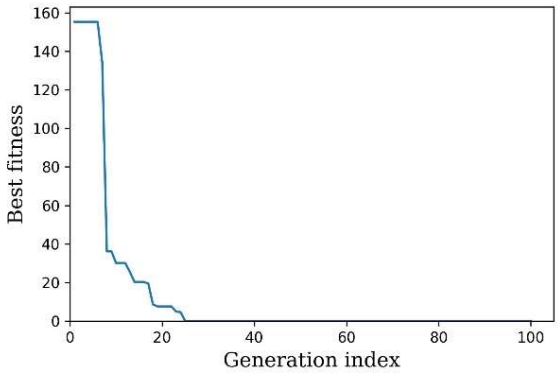

Fig. 5 Evolution graph of the GA on the balanced reinforcement ratio of a prestressed SFRC beam

Fig. 6 shows the variation of strain at the top layer of concrete and at the tensile reinforcement layers, for strain increments defined in DoCros software, considering the design values listed in Table 2. According to the design criteria, the yielding of steel strands occurred before concrete crushing ($\varepsilon_{cu} = 0.0035$) and the rupture of GFRP rebars occurred at the same time as concrete crushing. This difference can be recognized in the fitness value obtained from the GA output.

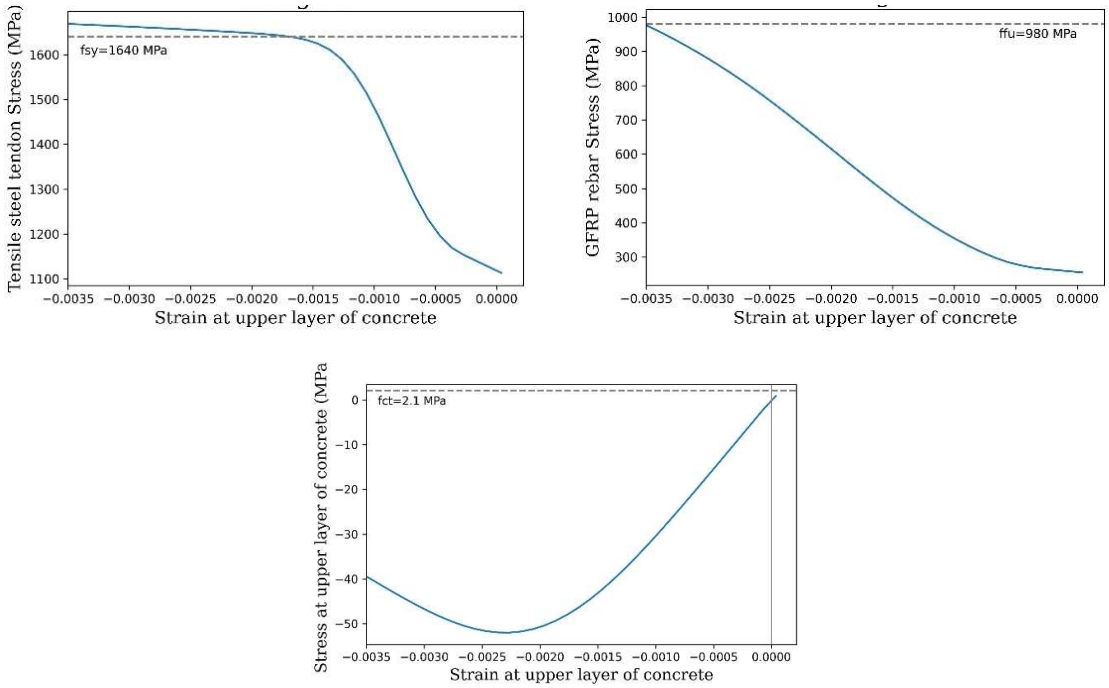

Fig. 6 Stress and strain evolution at tensile reinforcement for strain incremental iterations (Negative value means compression)

Fig. 7 shows the moment-curvature diagram of the designed beam. The nominal flexural strength of the beam is obtained from the maximum moment stage of the moment-curvature diagram of the cross-

section. The negative curvature in this diagram is caused by the internal moment induced by the prestress.

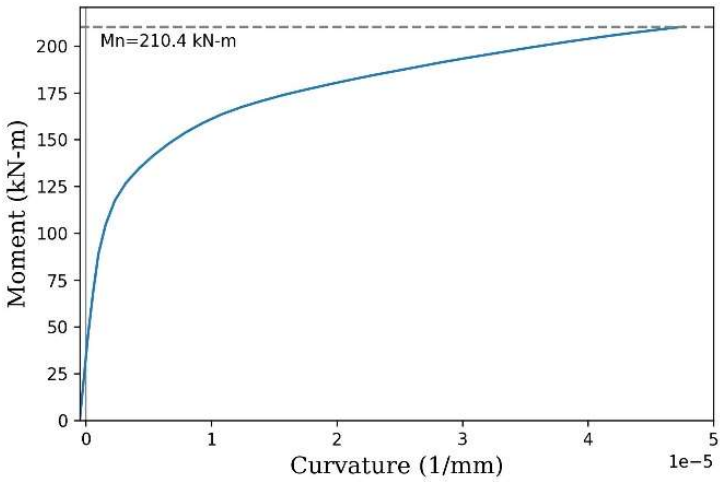

Fig. 7 Moment-curvature diagram of the designed beam

Deflection

Deflection of prestressed beams is divided into two categories: short-term or immediate, and long-term deflection. A short-term deflection is calculated for the immediately after the application of the design load cases/combinations, not taking into consideration the time-dependent deformability of concrete, and assuming the concrete behaves in an elastic stage. When considering long-term deflection, concrete time-dependent effects on its deformability must be considered, like creep and shrinkage.

According to Eurocode-2 (Européen, 2004), for the serviceability design, the deflection should not exceed the deflection limit that depends on the type of structure and its intended use. For instance, in the case of a car park floor, the deflection limit is span(mm)/250.

Force-deflection relationship

The force-deflection response is obtained by DefDoCros software for a 4-point loading flexural test with a loading distance of 500mm in the middle of the beam. The DefDoCros uses the moment-curvature relationship data derived from DoCros software and predicts the force versus deflection response of the prestressed SFRC beam by using the displacement method (Barros & Fortes, 2005). Fig. 8a shows the schematic representation of the loading and support conditions of this beam. The force-deflection responses of the designed beams up to the failure at the mid-span of the beam are plotted in Fig. 8b. In this figure the vertical line indicates a deflection of 15 mm, which is the deflection at service limit state condition for this beam.

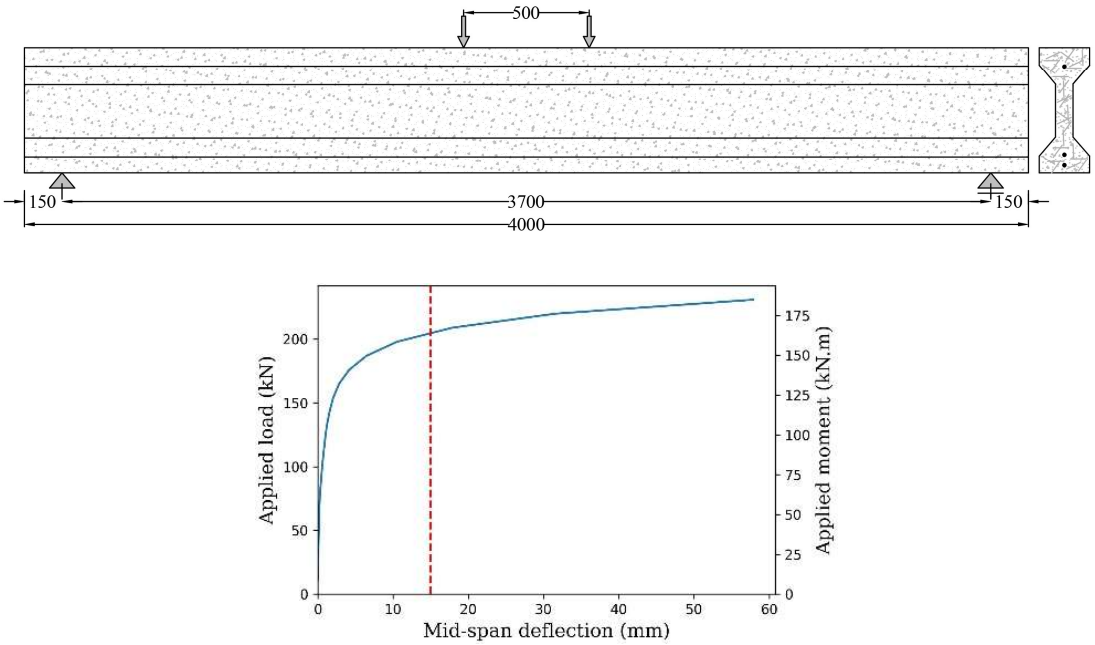

Fig. 8 (a) Loading and support conditions of the beam (b)Applied force versus mid-span deflection of the prestressed hybrid SFRC beam

CONCLUSIONS

The design process of a hybrid prestressed SFRC beam and its optimization method using a genetic algorithm have been discussed in this paper. It is demonstrated that the procedure can obtain the balanced reinforcement ratio for a given beam section.

In addition, the following conclusions can be drawn from this study:

- The outcome demonstrates how meta-heuristic algorithms may be used in the flexural design of prestressed hybrid SFRC beams.
- Due to the use of discrete design and probable design variable values, the GA reached realistic and applicable solutions.
- The present model doesn't require cumbersome formulas and experience-based guidelines of design.
- The proposed method using a moment-curvature diagram for the optimization can be used regardless of cross-sectional shape and material.

ACKNOWLEDGEMENTS

The first author gratefully acknowledges the financial support of "Fundação para a Ciência e Tecnologia" (FCT-Portugal), through the PhD grant SFRH/BD/09253/2020. The authors acknowledge the support provided by FCT through the project FemWebAI, reference PTDC/ECI-EST/6300/2020, and PID2021-125553NB-I00 (MCI/AEI/FEDER, UE). This work was partly financed by FCT / MCTES through national funds (PIDDAC) under the R&D Unit Institute for Sustainability and Innovation in Structural Engineering (ISISE), under reference UIDB/04029/2020, and under the Associate Laboratory Advanced Production and Intelligent Systems ARISE under reference LA/P/0112/2020.

CONFLICT OF INTEREST

The authors declare that they have no conflicts of interest associated with the work presented in this paper.

DATA AVAILABILITY

Data on which this paper is based is available from the authors upon reasonable request.

REFERENCES

Aashto, L. (2012). AASHTO LRFD bridge design specifications. *American Association of State Highway and Transportation Officials: Washington, DC, USA*.

Adel, M., Matsumoto, K., Ueda, T., & Nagai, K. (2022). Material comparative analysis of crack-bridging degradation of SFRC structural beams under flexural fatigue loading. *Construction and building materials*, *339*, 127642.

Ahmed, T., & Chidambaram, R. S. (2022). Shear strength of steel fiber reinforced concrete beam–A review. *Materials Today: Proceedings*.

Aydın, Z., & Ayvaz, Y. (2010). Optimum topology and shape design of prestressed concrete bridge girders using a genetic algorithm. *Structural and Multidisciplinary Optimization*, *41*(1), 151-162.

Barros, J. A., Costa, I. G., Frazão, C. M., Valente, T. D., Lourenço, L. A., & Melo, F. J. (2022). Innovative prefabricated lightweight slab system of high structural performance. *Engineering Structures*, *259*, 114146.

Barros, J. A., & Fortes, A. (2005). Flexural strengthening of concrete beams with CFRP laminates bonded into slits. *Cement and Concrete Composites*, *27*(4), 471-480.

Basto, C., & Barros, J. (2008). Numeric simulation of sections submitted to bending. *Department of Civil Engineering, School of Engineering, University of Minho Guimarães,, Portugal, Technical Report*.

Chen, C., Yang, Y., Zhou, Y., Xue, C., Chen, X., Wu, H., . . . Li, X. (2020). Comparative analysis of natural fiber reinforced polymer and carbon fiber reinforced polymer in strengthening of reinforced concrete beams. *Journal of cleaner production*, *263*, 121572.

El-Nemr, A., Ahmed, E. A., El-Safty, A., & Benmokrane, B. (2018). Evaluation of the flexural strength and serviceability of concrete beams reinforced with different types of GFRP bars. *Engineering Structures*, *173*, 606-619.

Européen, C. (2004). Eurocode 2: Design of concrete structures—Part 1-1: General rules and rules for buildings. *London: British Standard Institution*.

Gemi, L., Madenci, E., & Özkılıç, Y. O. (2019). An Investigation on Effect of Steel/Glass Fiber Bars in Concrete Beams. VI International Earthquake Symposium (IESKO 2019),

Giacomelli, D. (2018). *Geneticsharp Github*. GitHub repository. https://github.com/giacomelli/GeneticSharp

Lu, C., Cai, Q., Xu, K., Sha, X., & Yan, Y. (2022). Comparison of flexural behaviors between plain and steel-fiber-reinforced concrete beams with hybrid GFRP and steel bars. Structures,

Matos, L. M., Barros, J. A., Ventura-Gouveia, A., & Calcada, R. A. (2020). Constitutive model for fibre reinforced concrete by coupling the fibre and aggregate interlock resisting mechanisms. *Cement and Concrete Composites*, *111*, 103618.

Mazaheripour, H., Barros, J. A., Sena-Cruz, J., Pepe, M., & Martinelli, E. (2013). Experimental study on bond performance of GFRP bars in self-compacting steel fiber reinforced concrete. *Composite structures*, *95*, 202-212.

Mazaheripour, H., Barros, J. A., Soltanzadeh, F., & Sena-Cruz, J. (2016). Deflection and cracking behavior of SFRSCC beams reinforced with hybrid prestressed GFRP and steel reinforcements. *Engineering Structures*, *125*, 546-565.

Mirjalili, S. (2019). Genetic algorithm. In *Evolutionary algorithms and neural networks* (pp. 43-55). Springer.

Pan, Y., & Yan, D. (2021). Study on the durability of GFRP bars and carbon/glass hybrid fiber reinforced polymer (HFRP) bars aged in alkaline solution. *Composite structures*, *261*, 113285.

Rosa, I., Firmo, J., Correia, J., & Barros, J. (2019). Bond behaviour of sand coated GFRP bars to concrete at elevated temperature–Definition of bond vs. slip relations. *Composites Part B: Engineering*, *160*, 329-340.

Rossini, M., & Nanni, A. (2019). Composite strands for prestressed concrete: State-of-the-practice and experimental investigation into mild prestressing with GFRP. *Construction and building materials*, *205*, 486-498.

Salehian, H., & Barros, J. A. (2017). Prediction of the load carrying capacity of elevated steel fibre reinforced concrete slabs. *Composite structures*, *170*, 169-191.

Shahrbijari, K. B., Saha, S., Barros, J. A., Valente, I. B., Dias, S., & Leite, J. (2020). Development and Mechanical Characterization of Dry Fiber-reinforced Concrete for Prefabricated Prestressed Beams. RILEM-fib International Symposium on Fibre Reinforced Concrete,

Spagnuolo, S., Rinaldi, Z., Donnini, J., & Nanni, A. (2021). Physical, mechanical and durability properties of GFRP bars with modified acrylic resin (modar) matrix. *Composite structures*, *262*, 113557.

Taheri, M., Barros, J. A., & Salehian, H. (2020). Integrated approach for the prediction of crack width and spacing in flexural FRC members with hybrid reinforcement. *Engineering Structures*, *209*, 110208.

Varma, R., Barros, J. A., & Sena-Cruz, J. (2012). Design-curves of strain softening and strain hardening fibre reinforced concrete elements subjected to axial load and bending moments.